ELSEVIER

Contents lists available at ScienceDirect

Harmful Algae

journal homepage: www.elsevier.com/locate/hal





The cytotoxic and hemolytic potential of karmitoxin from *Karlodinium* armiger and how it interacts with sterols

Hélène-Christine Prause a,b, Nadine Hochmayr, Yanan Yu, Homas Ostenfeld Larsen, Per Juel Hansen, Giorgia Del Favero a,f, Doris Marko, Allen Place, Elisabeth Varga, A,h, La Borne, Nadine Hochmayr, Allen Place, Christine, Nadine Hochmayr, Yanan Yu, A,d, Thomas Ostenfeld Larsen, Per Juel Hansen, Giorgia Del Favero, Doris Marko, Allen Place, Elisabeth Varga, A,h, La Borne, Christine, Nadine Hochmayr, Anna Yu, C,d, Thomas Ostenfeld Larsen, Per Juel Hansen, Giorgia Del Favero, Doris Marko, Allen Place, Blisabeth Varga, Allen Place, Christine, Christi

- a Department of Food Chemistry and Toxicology, Faculty of Chemistry, University of Vienna, Währinger Str. 38-40, 1090 Vienna, Austria
- ^b Vienna Doctoral School in Chemistry, Faculty of Chemistry, University of Vienna, Währinger Str. 42, 1090 Vienna Austria
- c Department of Biotechnology and Biomedicine, Technical University of Denmark, Søltofts Plads 221, 2800 Kgs. Lyngby, Denmark
- d Key Laboratory of Oceanic and Polar Fisheries, Ministry of Agriculture and Rural Affairs, East China Sea Fisheries Research Institute, Chinese Academy of Fishery Sciences, Jungong Road 300, Shanghai, 200090, China
- ² Marine Biological Section, Department of Biology, University of Copenhagen, Strandpromenaden 5, 3000 Elsinore, Denmark
- f Core Facility Multimodal Imaging, Faculty of Chemistry, University of Vienna, Währinger Str. 38-42, 1090 Vienna, Austria
- g Institute of Marine and Environmental Technology, University of Maryland Center for Environmental Science, 701 E. Pratt Street, Baltimore, MD 21202, USA
- h Unit Food Hygiene and Technology, Centre for Food Science and Veterinary Public Health, Clinical Department for Farm Animals and Food System Science, University of Veterinary Medicine, Vienna, Veterinärplatz 1, 1210 Vienna, Austria

ARTICLE INFO

Keywords: Ichthyotoxin Mode of action Lysis Cholesterol RTgill-W1 HCEC-1CT

ABSTRACT

Karmitoxin, produced by Karlodinium armiger, is structurally related to karlotoxin and amphidinols, two potent ichthyotoxic hemolysins with high affinity for sterols. Given these structural similarities, karmitoxin is believed to exhibit comparable toxic effects. Cytotoxicity was assessed in the fish gill cell line RTgill-W1 and the human epithelial colon cell line HCEC-1CT. The hemolytic potential with and without added sterols was tested on fish erythrocytes to investigate possible impacts of toxin-sterol interactions. Sterol interactions were further evaluated using surface plasmon resonance. A 3-h incubation returned an EC₅₀ of 111 and 175 nM in RTgill-W1 and in HCEC-1CT cells, respectively. Lactate dehydrogenase (LDH) release increased with toxin concentration, reaching 11 % in the fish and 40 % in the human cell line. Extended exposure (24 h) increased the toxicity in RTgill-W1 cells (EC50 74 nM, 40 % LDH release). In parallel, hemolytic potential of karmitoxin was confirmed, as well as its interaction with free sterols. Interaction kinetics revealed complex stabilities with $k_d(s^{-1})$ constants of 1.13 × 10^{-2} (cholesterol), 5.48×10^{-3} (epicholesterol), and 4.72×10^{-3} (ergosterol). Interaction with cholesterol followed the single-exponential model well, while data indicated more complex binding with epicholesterol and ergosterol. Altering the RTgill-W1 cholesterol content did not impact cytotoxicity at the tested concentration. Overall, karmitoxin showed potent cytotoxic and hemolytic properties in human and fish models. Complex formation with sterols may play a role in membrane targeting, yet cellular cholesterol quantity might not affect cytotoxicity.

1. Introduction

The dinoflagellate species *Karlodinium armiger* was identified and isolated from the Mediterranean Sea two decades ago (Bergholtz et al., 2006; Garcés et al., 2006). This species has been associated with several fish kills and has since its discovery been found to produce an ichthyotoxin called karmitoxin which is structurally similar to karlotoxins and amphidinols (Fig. 1) (Rasmussen et al., 2017). The key feature

distinguishing karmitoxin from karlotoxin and amphidinols is the primary amine group at the end of the lipophilic arm. The mode of action (MOA) of karlotoxin and amphidinols is an ongoing area of research and is tentatively understood. It has been shown that these toxins can create pores in the plasma membrane, a process which is supported by their high affinity for membrane sterols, cholesterol or ergosterol (Deeds and Place, 2006; Deeds et al., 2002; Place et al., 2009; Swasono et al., 2010; Waters et al., 2015; Place et al., 2024). Their ability to create pores has

E-mail address: elisabeth.varga@vetmeduni.ac.at (E. Varga).

https://doi.org/10.1016/j.hal.2025.102817

^{*} Corresponding author.

H.-C. Prause et al. Harmful Algae 143 (2025) 102817

also been described to be largely aided by their hairpin structure, which all of these compounds have in common (Houdai et al., 2005; Waters et al., 2015). The information available on the MOA of karlotoxins and amphidinols may suggest that karmitoxin could likewise possess affinity towards cholesterol, and that its lytic potency is influenced by or dependent on the presence of cholesterol.

Therefore, the purpose of this project was to shed light on the interaction with sterols, particularly cholesterol, as well as on the importance of sterols in the MOA of karmitoxin. Interactions with different types of sterols were tested in hemolysis assays using blood from Atlantic salmon (Salmo salar) and were also assessed using surface plasmon resonance (SPR) to gain insight into the binding kinetics. Invitro cytotoxicity tests were performed in the rainbow trout gill cell line RTgill-W1 and the epithelial human colon cell line HCEC-1CT. This human cell line was selected to demonstrate that karmitoxin toxicity is not limited to fish gill cells. It may also provide insights into potential adverse effects in the event of human exposure to this ichthyotoxin. The effect of altering the cholesterol content of RTgill-W1 cells on the potential of karmitoxin was also assessed in cytotoxicity experiments.

2. Materials and methods

2.1. Algal culture and toxin purification

K. armiger strain K-0668 was acquired from the Scandinavian Culture Collection of Algae and Protozoa (SCCAP now part of Norwegian Culture Collection of Algae (NORCCA)). The algae were grown in modified f/2 medium with 50 μM NH₄, replacing NO₃, in autoclaved natural sea water at a salinity of 30. This was done according to the findings of Binzer et al. (2020), who showed that the mixotrophic algae K. armiger can grow well with the addition of NH₄⁺ as a food source. NaHCO₃ at a final concentration of 0.5 mM was added to media after autoclaving the sea water. Cultures were grown at a constant temperature of 15 $^{\circ}\text{C}$ with aeration, a light-dark cycle of 14:10 h, and an irradiance of 150 μ mol photons m⁻²·s⁻¹. Once the algae had reached stationary phase they were centrifuged, the supernatant was then loaded onto a C18 Sepra material (Phenomenex) in a SNAP column (60 g) and eluted with 80 % methanol containing 10 mM formic acid using an Isolera autoflash system (both Biotage, Uppsala, Sweden). Karmitoxin was then isolated by semipreparative HPLC on a Luna C18(2) column using an acetonitrile-H₂O gradient from 30 % to 50 % acetonitrile containing 50 ppm trifluoroacetic acid over 40 min at a flow rate of 4 mL/min. The purified karmitoxin was then reconstituted in ethanol (EtOH) and the protocol using high performance liquid chromatography and fluorescent detection (HPLC-FLD) for toxin semi-quantitation described for prymnesins by Svenssen et al. (2019) was applied to estimate the karmitoxin concentration. In short, the primary amine of karmitoxin was derivatized

through labeling with a fluorescent tag (AccQ-Tag Fluor Reagent Kit, Waters Corporation, Milford, MA, USA). The chromatographic separation was performed on a 1200 HPLC system (Agilent Technologies, Waldbronn, Germany), using an Agilent Poroshell C18 column (2.1 \times 50 mm, 2.7 μm) using water (0.1 % formic acid) as eluent A and acetonitrile (0.1 % formic acid) as eluent B. The toxin was detected at a fluorescence excitation wavelength of 250 nm and an emission wavelength of 395 nm. Data were evaluated using ChemStation for LC Rev. B.04.01 SP1 from Agilent Technologies.

2.2. Cell culture

Cell viability tests were mainly performed on the rainbow trout (*Oncorynchus mykiss*) gill cell line RTgill-W1. This cell line was provided by K. Schirmer, Department of Environmental Toxicology, EAWAG, Dübendorf, Switzerland. Cultivation was performed as previously described, at 19 °C in Leibovitz's 15 medium (L-15) supplemented with 1 % (ν/ν) penicillin/streptomycin (Thermo Fisher Scientific, Waltham, MA, USA) and 10 % (ν/ν) fetal calf serum (EuroBio, Le Ulis, France) (Bols et al., 1994).

Cytotoxicity tests were also conducted on the human epithelial colon cell line HCEC-1CT, which was kindly provided by J.W. Shay, UT Southwestern Medical Center, Dallas, TX, USA, and cultured at 37 °C and 5 % CO₂. Cultivation medium was prepared with 500 mL Dulbecco's Modified Eagle's Medium (DMEM (Thermo Fisher Scientific, Waltham, MA, USA)) supplemented with 10 mL HEPES buffer solution 1 M, 10 mL Medium 199 (10x), 10 mL HyClone™ Cosmic Calf™ Serum (GE Healthcare Life Sciences HyClone Laboratories, Danaher Corporation, Washington DC, USA), 5.2 mL Insulin-Transferrin-Selenium-G Supplement (Thermo Fisher Scientific, Waltham, MA, USA), 0.6 mL gentamycin solution (Sigma Aldrich GmbH, St. Louis, MO, USA), 100 μL Recombinant Human Epidermal Growth Factor (100 μg/mL, Szabo-Scandic HandelsgmbH & Co KG, Vienna, Austria), and 100 μL hydrocortisone (5 mg/mL, Merck KGaA, Darmstadt, Germany).

2.3. Toxicity assays

2.3.1. Hemolytic assay

The hemolytic potential of karmitoxin was evaluated using red blood cells (RBCs) obtained from Atlantic salmon ($Salmo\ salar$). The protocol for preparation of the buffers and the RBC-solution was adapted from Deeds et al. (2002) and followed as described in Prause et al. (2024). Briefly, heparin-treated needles were used to draw blood, which was subsequently centrifuged at 1250 rcf and 4 °C for 25 min and washed with Tris-buffer I, consisting of 150 mM NaCl, 3.2 mM KCl, 1.25 mM MgSO₄, 12.2 mM Tris base in MilliQ water. A 1.25 % (ν/ν) RBCs solution in Tris-buffer II (Tris-buffer I+ 3.75 mM CaCl₂) was prepared and stored

Karnitoxin

$$H_2N$$
 OH
 OH

Fig. 1. Structures of karmitoxin produced by the dinoflagellate Karlodinium armiger in comparison to karlotoxin 2 from Karlodinium veneficum and amphidinol 3 from Amphidinium klebsii.

at 4 °C for up to 10 days. The pH of both buffers was adjusted before sterile filtration (0.22 μm) to pH 7.4 at 10 °C, and a hemolytic calibration curve using saponin (Quillaja bark, CAS No.: 8047-15-2; Sigma Chemical Co., St. Louis, MO, USA) was created for each new batch of 1.25 %-RBC solution. The stability of the RBC solution was monitored by observing the absorbance value obtained for incubation with only Tris-buffer II. Saponin (8 µg/mL) was also used as positive control, and the solvent control consisted of Tris buffer II containing 0.5 % (v/v)EtOH. The assays were carried out in 96-well plates (V-bottom, polystyrene, non-treated, Corning Inc., Corning, NY, USA). All experiments involving fish were carried out in accordance with the guidelines at the Institutional Animal Care and Use Committee (IACUC) of the University of Maryland Medical School: protocol No 0014 and No 0522012. Fish used for tissue sampling were anesthetized with tricaine methanesulfonate (MS-222, 10 mg/L) for blood sampling and then euthanized with MS-222 (150 mg/L).

2.3.2. CellTiter blue® (CTB)

The CellTiter Blue® (CTB, (Promega, Madison, WI, USA)) assay was used to determine the cytotoxicity of karmitoxin on RTgill-W1 and HCEC-1CT cells. Cells were seeded onto 96-well plates at a density of 2×10^4 cells per well (RTgill-W1) or 5×10^3 cells per well (HCEC-1CT). Following a 48-h growing period, they were exposed to karmitoxin diluted in culture medium (final EtOH concentration $0.5\%~(\nu/\nu)$). The solvent control consisted of medium containing $0.5\%~(\nu/\nu)$ EtOH, and the positive control was 0.05% and 0.1% Triton $^{\rm TM}$ X-100 (Triton X, (Sigma-Aldrich, St. Louis, MO, USA)) in culture medium. The cells were incubated with karmitoxin for 3 or 24 h in the dark at 19 °C (RTgill-W1) or 37 °C (HCEC-1CT). Subsequently, the solutions were aspirated and $100~\mu$ L 1:10 diluted CTB reagent in the respective culture medium was added to the cells. After a 1-h reaction time, 80 μ L of the CTB-supernatant were transferred into a black 96-well plate and fluorescence was measured according to the manufacturer's instructions.

2.3.3. Lactate dehydrogenase (LDH) assay

Lytic effects of karmitoxin were assessed with the lactate dehydrogenase (LDH) assay (Pierce CyQuant $^{\rm TM}$, Thermo Scientific, Waltham, MA, USA). The manufacturer's protocol was followed. Briefly, after the 3-h toxin incubation 50 μL supernatant were transferred onto a new F-bottom 96-well plate, and by adding 50 μL LDH reaction mix the reaction was initiated. After 30 min 50 μL stop solution were added and the absorbance was read at 490 and 680 nm.

2.4. Interaction with sterols

2.4.1. Sterol combinations

In order to understand whether karmitoxin can interact with sterols, cholesterol (5(6)-cholesten-3-ol, Sigma St. Louis, MO, USA) and epicholesterol (5-cholesten-3a-ol, Steraloids Inc., Newport, RI, USA) were combined with karmitoxin before starting a hemolytic assay. The selection of these sterols was based on previous work showing that karlotoxin built highly stable complexes with cholesterol, but not with its epimer epicholesterol (Place et al., 2024). The assay protocol of Prause et al. (2024) was followed. Shortly, the karmitoxin sample diluted to the HC_{50}^{-1} value was combined with the equivalent volume of either one of the sterols ranging from 0.1 nM to 10,000 nM. Sterols had previously been dissolved in EtOH, and dilutions were performed to maintain a total EtOH concentration of 0.5 % (ν/ν). Hemolysis was performed as described previously, by adding 100 μ L 1.25 % (ν/ν) RBC solution.

2.4.2. Surface plasmon resonance (SPR)

Binding interactions of karmitoxin with cholesterol, epicholesterol, and ergosterol (Fluka Chemie GmbH, Buchs, Switzerland) were also

recorded via surface plasmon resonance (SPR). The protocol, originally described by Place et al. (2024) was followed precisely, using the T200 Biacore system with a Series S Sensor Chip HPA (Cytiva, Danaher Corporation, Washington, DC, USA). The flow cells (Fcs) of the sensor chip were first pre-conditioned with 40 mM octyl-d-glucoside for 5 min at a flow rate of 10 μ L/min. The sterols were diluted to 10 μ M in HBS buffer (10 mM HEPES, 150 mM NaCl, pH 7.4) and immobilized on the Fcs at about 1000 responsive units (RUs) with a flowrate of 2 µL/min for 30 min. The Fcs were rinsed with 10 mM NaOH for 30 s and then blocked for 5 min using bovine serum albumin (0.1 mg/mL in dH₂O). HBS buffer was run over the sensor chip three times before karmitoxin at 1 μM was run over the Fcs for 2 min at 10 $\mu L/\text{min}.$ The responses were fitted on a 1:1 model, and complex stabilities were evaluated by calculating the dissociation rate constant k_d(s⁻¹) with the program Biacore T200 Evaluation Software version 3.2.1 (Cytiva, Danaher Corporation, Washington, DC, USA).

2.4.3. Membrane cholesterol in RTgill-W1 cells

To get a better understanding of the relevance of cholesterol in the cytotoxic potential of karmitoxin the cholesterol content of the cells was modified to contain more or less cholesterol as described in Prause et al. (2024). A 24-h cholesterol-altering treatment was conducted using 10 μM lovastatin (lovastatin sodium salt, Enzo, Farmingdale, NY, USA) for depletion and 10 μM methyl- β -cyclodextrin (MbCD) loaded with cholesterol (MbCD-Chol (Sigma Aldrich GmbH, St. Louis, MO, USA)) to augment cholesterol contents (Del Favero et al., 2020; Rebhahn et al., 2022). The cellular cholesterol content was relatively quantified via fluorescence microscopy as reported in the previous paper, and a total cholesterol increase of about 30 % and a decrease of approximately 25 % could be achieved (Prause et al., 2024). Following the 24-h treatment, karmitoxin at approximately EC80 was added to the cholesterol-modified as well as unaltered cells and incubated for 3 h. The resulting cell viability was measured via CTB assay.

2.5. Statistics

All assays were carried out in technical triplicates, with the exception of SPR assays, which were performed in duplicates. The number of biological replicates is provided below the figures. Significance (* = p < 0.05; ** = p < 0.01; *** = p < 0.001) was calculated with One Way ANOVA followed by the posthoc Fisher's least significant difference test, as well as *t*-test (one-sample or two-sample) using OriginPro 2020 Version 9.7.0.185 (Academic) from OriginLab Corporation (Northampton, MA, USA). RStudio version 4.0.2 (RStudio Inc., Boston, MA, US) was used for calculating EC $_{50}$ values.

3. Results

3.1. Toxicity

3.1.1. Hemolytic activity

Karmitoxin was tested for hemolysis of RBCs obtained from salmon blood. Concentrations ranging from 15 – 240 nM were applied to obtain a hemolytic response curve (Fig. 2). Strong hemolytic potential was observed, and an HC $_{50}$ value of 160 nM could be estimated. The highest concentration, 290 nM, caused 90 % hemolysis of RBCs.

3.1.2. Cytotoxicity and lytic activity in RTgill-W1 cells

RTgill-W1 cells were used to assess the cytotoxic potential of the karmitoxin sample for both 3-h and 24-h exposure. Following a 3-h incubation (Fig. 3A) a linear decline in the metabolic activity was measured, with a 50 % cell viability (EC $_{50}$) achieved by approximately 111 nM karmitoxin. The release of intracellular LDH was positively correlated to cytotoxicity, with the largest release (about 11 %) at the highest tested concentration (191 nM). The first significant reduction in metabolic activity was observed at 78 nM karmitoxin, yet the first

¹ Concentration at which 50 % of all RBCs are lysed.

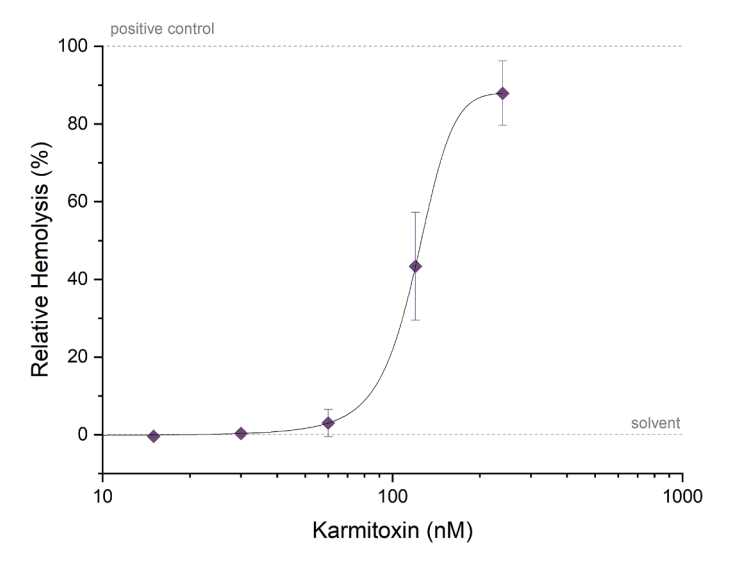


Fig. 2. Hemolytic activity of karmitoxin in erythrocytes of Atlantic salmon (*Salmo salar*). Saponin (8 µg/mL) was used as positive control and set as 100% hemolysis, Tris-buffer II containing 0.5% (ν/ν) EtOH was used as solvent control. Data is given as mean \pm SD of n = 3 biological replicates fitted on a nonlinear dose-response using the Levenberg Marquardt algorithm.

concentration at which a significant LDH release was observed was 122 nM. A 24-h incubation (Fig. 3B) was performed and compared to the standard incubation time of 3 h. The three lowest concentrations (40, 50, and 63 nM) caused an increase in metabolic activity to about 150 %, yet the higher concentrations (78 nM onwards) exhibited significantly stronger cytotoxic effects compared to the 3-h incubation. Exposure to 122 nM karmitoxin for 24 h decreased the metabolic activity by about 95 %, while a 3-h exposure only resulted in a 60 % reduction. The calculated corresponding EC50 for the 24-h incubation was thus approximately 74 nM. Interestingly, LDH release did not exceed 40 %, even at the highest concentrations of karmitoxin where the relative metabolic activity was at 0 %. In fact, the extracellular LDH content dropped back to 20 % at the highest concentration.

3.1.3. Cytotoxicity and lytic activity in HCEC-1CT cells

The cytotoxic potential of karmitoxin was also evaluated in a human cell line for the first time (Fig. 4). A slightly higher concentration range, from 80 nM to 382 nM, needed to be applied to the cells for the standard incubation time of 3 h. These concentrations were based on preliminary assays, demonstrating a lower sensitivity of this cell line towards karmitoxin. Both CTB and LDH measurements were performed. Interestingly, the cellular metabolic activity increased when exposed to the two lowest concentrations (80 nM and 100 nM), with no LDH release. A significant decrease in cell viability, to 30 % metabolic activity, was first observed at 196 nM. This concentration had reduced metabolic activity to about 10 % in RTgill-W1 cells. The first significant LDH leakage of 24 % from HCEC-1CT cells also took place after incubation with 196 nM karmitoxin. A concentration of approximately 300 nM was needed to achieve 0 % metabolic activity in HCEC-1CT cells. The highest LDH release of about 40 % occurred at 245 nM. This level of release remained consistent for the two subsequent highest concentrations tested (306 nM and 382 nM). The calculated EC_{50} value for karmitoxin in this cell line was approximately 175 nM.

Morphological changes of the cells after exposure to karmitoxin were observed in bright field images (Fig. 5). Upon coming in contact with karmitoxin the cells would change their shape and become more rounded, and with increasing concentrations the cells started detaching from the well bottom (Fig. 5A). Cells for which no metabolic activity was measured were generally presumed to be dead, which was supported by their swollen appearance and the fact that they had fully detached from

the well bottom. This can be observed for exposure of HCEC-1CT cells to 382 nM karmitoxin (Fig. 5B).

3.2. Sterol interactions

3.2.1. Combination assays

Whether karmitoxin can interact with sterols was evaluated by combining the toxin at its HC_{50} with different concentrations of cholesterol or epicholesterol. It was hypothesized that an interaction would subsequently affect the hemolytic potential (Place et al. 2024). Once the sterols were combined with the toxin, the expected 50 % hemolysis was reduced to 0 % with cholesterol, and nearly 0 % with epicholesterol (Fig. 6). This outcome was irrespective of the sterol concentration. Neither sterol exhibited hemolytic effects at any of the applied concentrations (supplementary information (SI) Fig. 1).

3.2.2. Surface plasmon resonance (SPR)

Following the hemolytic combination assays, the interaction between karmitoxin and sterols was studied more closely via SPR (Fig. 7). The T200 Biacore Evaluation Software (Cytiva, Danaher Corp., Washington, DC, USA) was used for the calculation of the dissociation rate constant $k_d(s^{-1})$, which can be used to interpret complex stability. Karmitoxin bound to all three sterols, and to octyl-d-glucoside (control) most likely due to an amphipathic character, as described for the structurally very close karlotoxin (Van Wagoner et al., 2008). Differences were observed between the three sterols, with $k_d(s^{-1})$ values of 1.13×10^{-2} for cholesterol, 5.48×10^{-3} for epicholesterol, and 4.72×10^{-2} 10⁻³ for ergosterol. From these constant rates it can be inferred that karmitoxin-cholesterol complexes decayed more quickly than the complexes formed with ergosterol or epicholesterol. The dissociation from ergosterol and epicholesterol on the other hand was nearly equal. The difference between the three sterols was further highlighted by the different fit quality (Chi²) of the single exponential model. Karmitoxin-cholesterol complexes seemingly followed this model well (Chi²(RU²) of 5.29), while the fitting of the karmitoxin-epicholesterol or -ergosterol complex decay exhibited larger Chi² values, indicating more intricate binding interactions.

3.2.3. Membrane cholesterol in RTgill-W1 cells

Considering that karmitoxin supposedly binds to membrane cholesterol and the high complex stability obtained via SPR, it was of interest to see whether altering the cholesterol content of RTgill-W1 cells would impact its cytotoxicity. Indeed, effective modification of the lipid can be achieved by treating the cells with either MbCD-Chol (10 μM) to augment, or lovastatin (10 μM) to reduce cholesterol content. This treatment and a subsequent relative quantification of the cellular cholesterol was previously reported in Prause et al. (2024), where the cholesterol content could be increased by approximately 30 % and lowered by about 25 %. The cells were then exposed to karmitoxin at approximately EC80 (approximately 160 nM) for 3 h. There was seemingly no difference between the cells regarding the impact on the metabolic activity (Fig. 8). A tendency for both treatments to exhibit a protective effect on the cells could be seen, but no significance could be calculated.

4. Discussion

Karmitoxin is considered a very potent hemolysin, and its structural similarity to karlotoxin and amphidinols serves as a key feature in understanding its chemical as well as functional and toxic properties (Rasmussen et al., 2017; Waters et al., 2015; Place et al. 2024). The cytotoxic potential of karmitoxin has already been established in previous studies using the RTgill-W1 cell line (Binzer et al., 2020; Rasmussen et al., 2017). The EC $_{50}$ of 111 nM for a 3-h incubation obtained in this work was similar to the 125 nM found by Rasmussen et al. (2017). In general, exposure of RTgill-W1 cells to karmitoxin for 24 h led to

H.-C. Prause et al. Harmful Algae 143 (2025) 102817

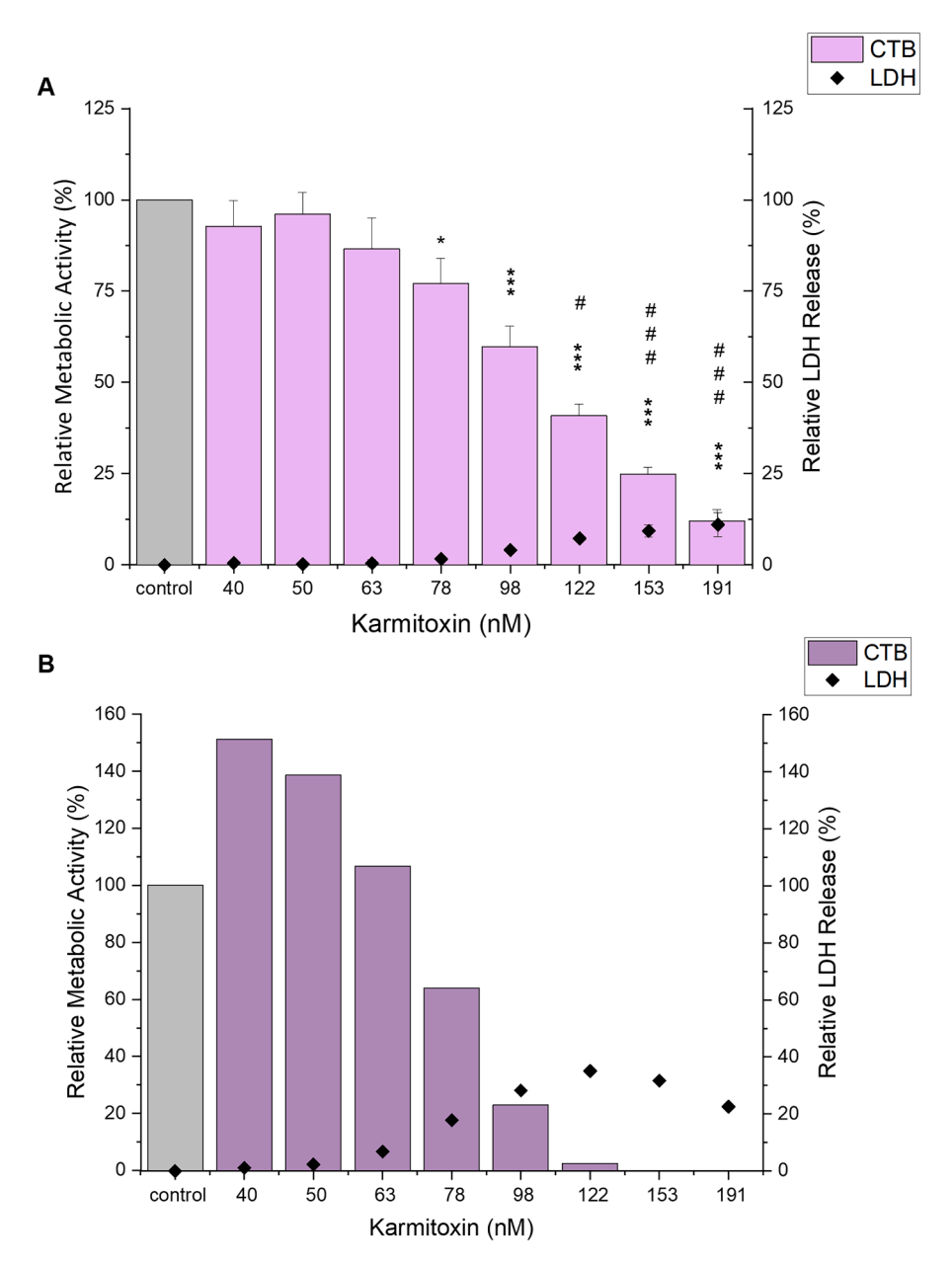


Fig. 3. Cytotoxic potency of karmitoxin in RTgill-W1 cells after 3h (A) and 24h (B), measured as metabolic activity of the cells via the CellTiter-Blue® (CTB) assay and the lactate dehydrogenase (LDH) assay. Medium containing 0.5% (ν/ν) EtOH was used as solvent control (100% for the CTB assay and 0% for the LDH assay). Data from A is presented as mean \pm SD of n \geq 4 biological replicates, significant differences between the measurements are labeled with * (CTB) or # (LDH). Normal distribution of the data was analyzed with the Shapiro-Wilk normality test (p < 0.05). Outliers according to Nalimov were eliminated. Data from B represent results of technical triplicates, therefore, no statistics were performed.

apparently stronger cytotoxicity, with a lower concentration (74 nM) reaching a 50 % decrease in metabolic activity. Interestingly, the metabolic activity resulting from 24-h exposure to the lower toxin range was drastically higher than the control, with close to no LDH release. This behavior could be attributed to activation of repair mechanisms aimed at maintaining cellular homeostasis as a response to stress induced by karmitoxin (Fulda et al., 2010; Welch, 1993). It can be assumed that lower concentrations of karmitoxin contributed to cellular stress, initiating a pro-survival signaling pathway. However, once a certain threshold is surpassed, either due to the severity or persistence of the stress factor, cells are no longer able to counteract the damage and switch to a cell death signaling pathway (Fulda et al., 2010). This phenomenon explains the higher metabolic activity measured for the lower concentrations of karmitoxin after 24 h compared to the 3-h incubation time. The activation of such repair mechanisms may not be immediate,

resulting in an initial disruption on cellular homeostasis (as observed after 3 h), which can later be repaired by the cellular stress response (as observed after 24 h).

The human epithelial cell line seemed to be less sensitive towards karmitoxin, with an EC $_{50}$ value of 175 nM compared to 111 nM in RTgill-W1 cells. It should be noted that cell numbers for seeding were selected based on their ability to reproduce and create a 100 % confluent monolayer within 48 h, in order to maintain testing conditions across both cell lines. As HCEC-1CT cells reproduce more quickly than RTgill-W1 cells, a lower cell number is required to reach confluence. Still, both values are comparable to each other as well as to the hemolytic potential towards Atlantic salmon RBCs, with an HC $_{50}$ of approximately 160 nM karmitoxin. Since membrane damage was also measured in RTgill-W1 and HCEC-1CT cells, it can be assumed that the cytotoxic effects were at least in part caused by lytic activity of karmitoxin. Surprisingly, the

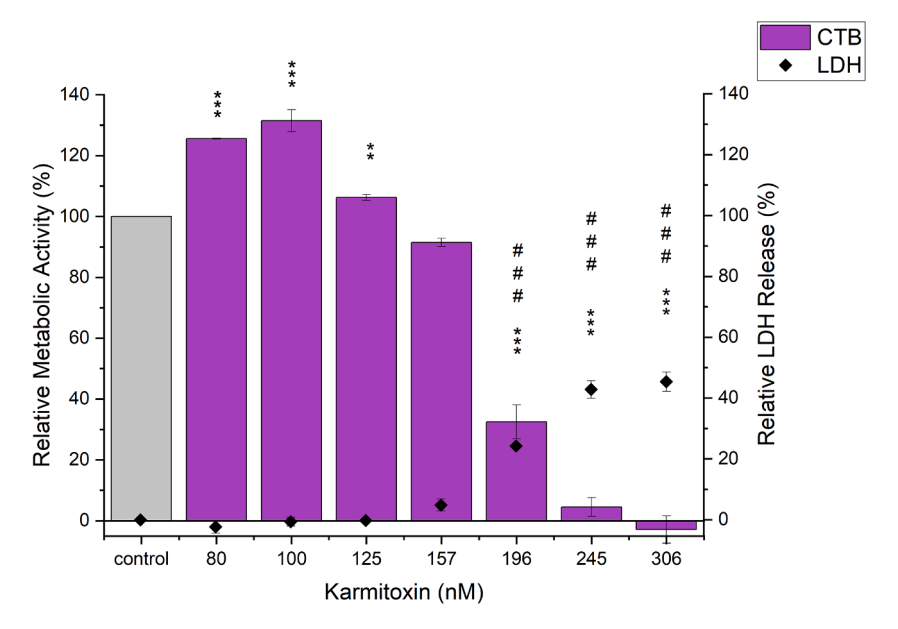


Fig. 4. Cytotoxic potency of karmitoxin in HCEC-1CT cells after 3 h, measured as metabolic activity of the cells via the CellTiter-Blue® (CTB) assay and the lactate dehydrogenase (LDH) assay. Medium containing 0.5 % (ν/ν) EtOH was used as solvent control (100 % for the CTB assay and 0 % for the LDH assay). Data is given as mean \pm SD of n = 3 biological replicates. Significant differences between the measurements are labeled with * (CTB) or # (LDH). Normal distribution of the data was analyzed with the Shapiro-Wilk normality test (p < 0.05). Outliers according to Nalimov were eliminated.

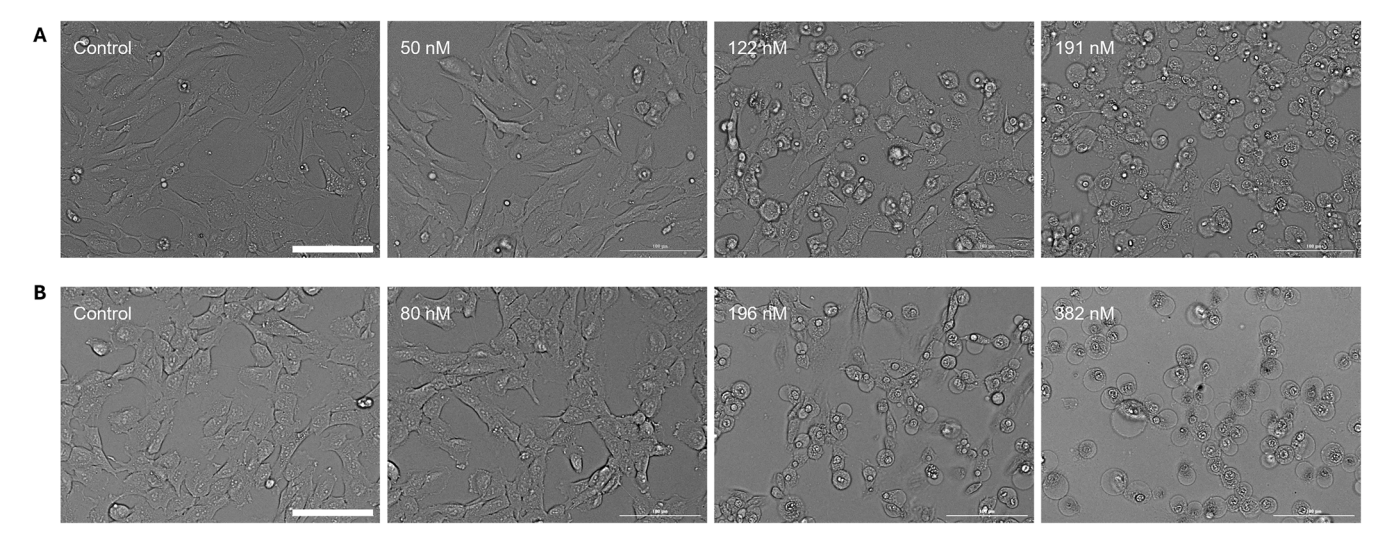


Fig. 5. Bright field images of RTgill-W1 cells (**A**) and HCEC-1CT cells (**B**) after 3-h exposure to various concentrations of karmitoxin in comparison to the control. The control consisted of the respective culture medium containing 0.5 % (ν/ν) EtOH. Image contrast and brightness were adjusted for better visibility. Scale bars represent

LDH release in both cell lines was much lower than expected, despite the positive control that represented the amount of LDH released from fully lysed RTgill-W1 or HCEC-1CT cells.

The enzyme LDH plays an essential role in the anaerobic breakdown of glucose, and its cellular levels may be impacted by the activation of pro-survival signaling pathways, which demand increased energy from cells (Brooks et al., 1999). This rationale may in part account for the low LDH values of cells exposed to high toxin concentrations, although it appears to be an oversimplification of this phenomenon. Despite an initial decrease in metabolic activity at the lower toxin concentrations, no LDH release was observed. LDH release increased only at higher concentrations, suggesting that higher toxin concentrations may stabilize or enlarge pore diameter, thereby delaying LDH release relative to metabolic effects. Furthermore, pore-formation may not be the only mechanism causing the cell death. A premise that might be supported by

the morphological state of the cells. To test this hypothesis, assays providing more information on cellular processes, such as cell cycle analyses, or monitoring dysregulation of cell signaling pathways including endoplasmic reticulum stress or oxidative stress are necessary (Fulda et al., 2010). Another option would be staining cellular structures such as cytoskeleton, nuclei, or mitochondria, to monitor changes thereof. Deeds et al. (2015) showed that karlotoxin can cause a non-selective pre-lytic increase in cellular cations. It may be that karmitoxin behaves in a similar way.

Generally, these results showed a rapid onset of cytotoxic effects induced by karmitoxin, which can be enhanced by longer incubation time, and possibly also reversed given that the concentration is low enough. This implies that the duration of toxin-exposure could impact the overall toxicity in the target organism. It would be of interest to assess whether RTgill-W1 cells exposed to karmitoxin, at various

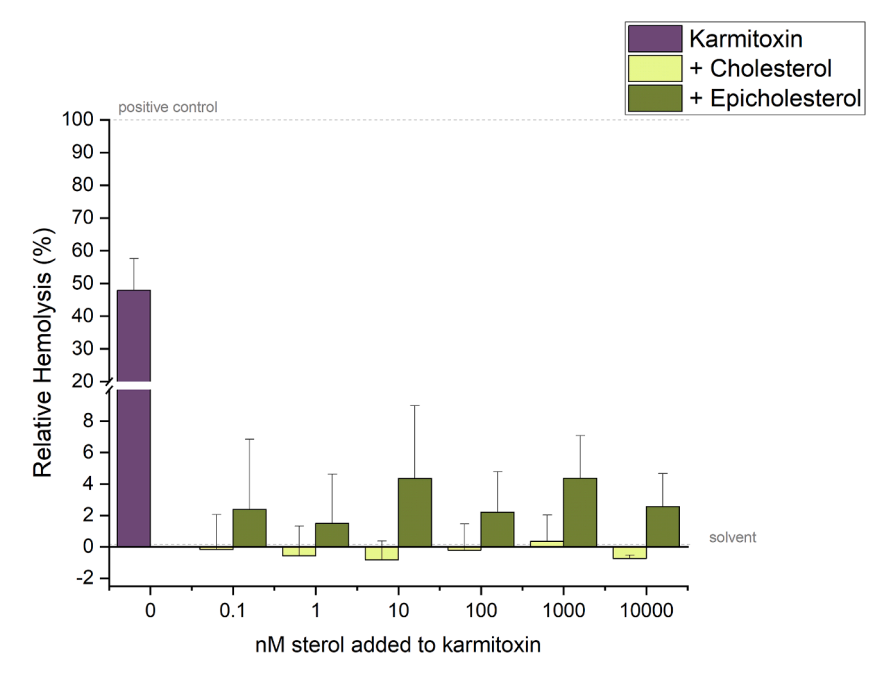


Fig. 6. Hemolytic potential of karmitoxin at HC_{50} (approximately 160 nM) compared to hemolytic effects resulting from combination of karmitoxin at HC_{50} combined with cholesterol or epicholesterol at different concentrations. Saponin (8 μ g/mL) was used as positive control and set as 100 % hemolysis, Tris-buffer II containing 0.5 % (ν / ν) EtOH was used as solvent control. Data is given as mean \pm SD of n=2 for cholesterol and n=3 for epicholesterol.

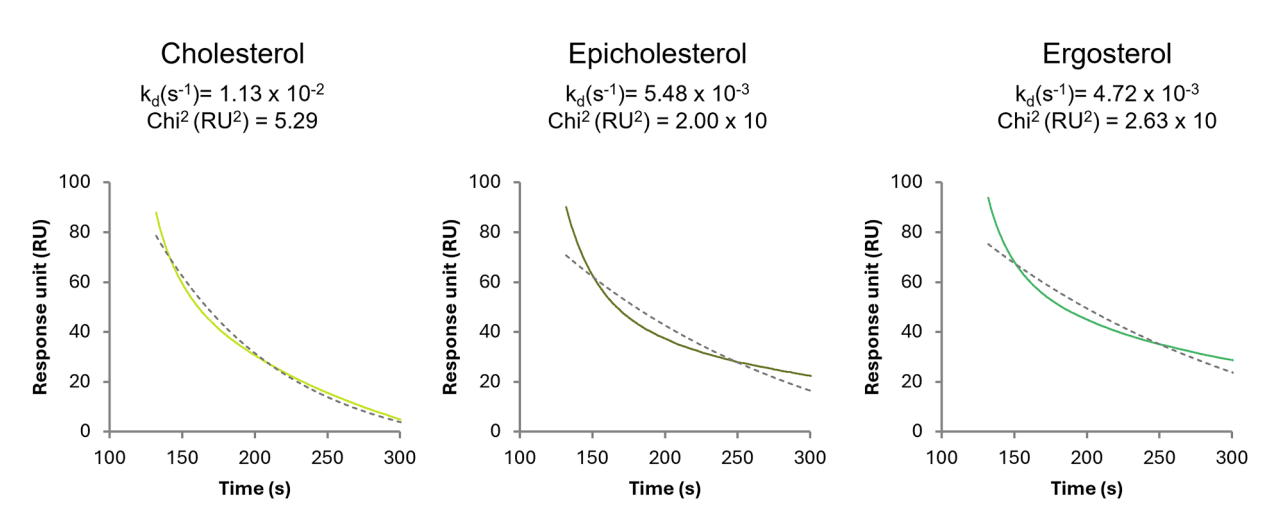


Fig. 7. Sensograms for 1 μ M karmitoxin binding to immobilized ligands; 10 mM cholesterol, 10 mM epicholesterol, and 10 mM ergosterol. The measured curves are shown in a solid line in color and the fitted curves in a dark gray dashed line. Measurements were performed in duplicates. The dissociation rate constant $k_d(s^{-1})$ and the quality of the fitted model $Chi^2(RU^2)$ are provided above the graphs.

concentrations and duration times, can recover from the cytotoxic damage during a recuperation period in toxin-free medium. This evaluation would help determine the efficacy of cellular repair mechanisms and identify a concentration threshold for successful repair. With information from such an *in-vitro* experiment it might be easier to estimate how fish would recover from short-term exposure to karmitoxin, similar to fish exposed to prymnesins from the haptophyte *Prymnesium parvum* (Svendsen et al., 2018). Importantly it could elucidate until which concentration such a recovery would be feasible.

The hemolytic potency of karmitoxin was similar to that of karlotoxin, albeit karmitoxin seemed to be more potent (Deeds et al., 2015). To lyse about 90 % of salmon RBCs, 290 nM karmitoxin were sufficient, yet 500 ng/mL (\approx 370 nM) karlotoxin 2 were necessary to lyse 90 % of trout RBCs (Deeds et al., 2015). We hypothesize that the unique amine group at the lipophilic arm of karmitoxin may be the reason for its stronger potency (Rasmussen et al., 2017). As a result, interaction with

phospholipids may be increased in comparison to karlotoxin, which would facilitate the insertion of karmitoxin into the cellular membrane (Place et al., 2009; Rasmussen et al., 2017). Of course, it should be noted that physiological differences between the RBC sources (salmon vs. trout) may exist. The combination of karmitoxin with sterols lowered the expected hemolysis significantly. This effect had already been documented for karlotoxin 2 in trout RBCs (Deeds and Place, 2006). No difference could be observed between the effects of cholesterol or epicholesterol. These results were corroborated by the SPR data, which showed that complex stabilities with cholesterol and epicholesterol were comparable, with dissociation rate constants of 1.13×10^{-2} s⁻¹ and 5.48 \times 10⁻³ s⁻¹, respectively. These k_d(s⁻¹) values are similar to the ones previously obtained for karlotoxin 2 and amphidinol 18 interacting with cholesterol (2.45 \times 10⁻³ s⁻¹ and 1.69 \times 10⁻² s⁻¹, respectively) (Place et al., 2024). Interestingly, the lowest dissociation rate was found for the complex with ergosterol, the main membrane sterol in fungi (Axelsson

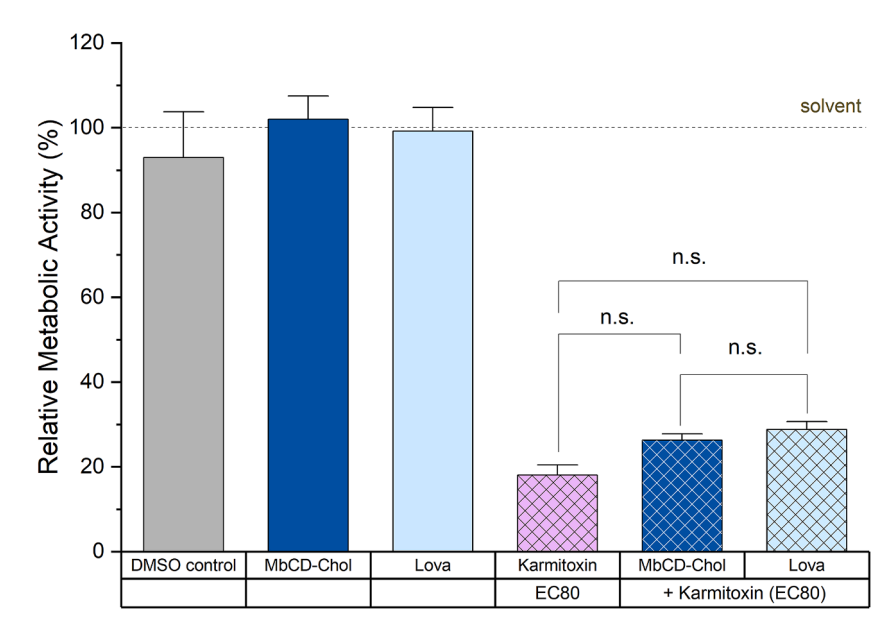


Fig. 8. Metabolic activity of regular and cholesterol-altered RTgill-W1 cells after 3-h exposure to karmitoxin at approximately EC₈₀ (approximately 160 nM). Methylβ-cyclodextrin loaded with cholesterol (MbCD-Chol, 10 μ M) was used to increase, and lovastatin (Lova, 10 μ M) to lower cellular cholesterol. Culture medium containing 0.5 % (ν / ν) EtOH served as solvent control and medium containing 0.25 % (ν / ν) dimethyl sulfoxide (DMSO) was used as solvent control for the Lova treatment. No significant difference between the karmitoxin treatments could be measured (n.s.). Data represent the mean \pm SD of n = 3 biological replicates.

et al., 1995; Dufourc, 2008). Amphidinols and karlotoxins have both been described as potent antifungal agents (Place et al., 2009; Satake et al., 1991; Van Wagoner et al., 2008). For amphidinols the strong affinity towards ergosterol was recently shown to be correlated to their antifungal potency (Matsumori et al., 2024; Swasono et al., 2010). With this information in mind, it can be assumed that karmitoxin also possesses antifungal capacities, and that these are likewise related to their affinity to ergosterol. Matsumori et al. (2024) also showed that amphidinol 3 seems to follow a 2-step reaction model. The authors proposed that the first binding step reflects sterol recognition and binding to the surface, while the second step, which the presence of ergosterol affected significantly more, represents an orientational change and most likely pore-formation (Matsumori et al., 2024). Based on the SPR results obtained here it could be argued that also karmitoxin follows a 2-step binding with ergosterol and epicholesterol.

Possibly the most unexpected result was that alteration of the cholesterol content of RTgill-W1 cells had no impact on the cytotoxic potency of karmitoxin. This indicates that sufficient cholesterol was still present in the membrane, allowing karmitoxin to target the cell membrane regardless of the $\sim\!25$ % decrease in cholesterol. As discussed in Prause et al. (2024), sterol modulation may take place throughout the entire cell, and not specifically in the cell membrane (Lange et al., 2004). This would mean that the actual change in membrane cholesterol was probably smaller than the measured 25 %. It is also likely that only small amounts of cholesterol are necessary for karmitoxin to target the cell membrane, just as it is likely for karmitoxin to interact with other lipids in the plasma membrane, such as the phospholipids. Regardless, both the increase and decrease of cholesterol resulted in the same tendency for somewhat lower cytotoxicity, which should be further examined. Creating liposomes with different sterol compositions would be valuable in assessing the significance of sterols for the MOA. Calcein leakage experiments previously performed for amphidinols have shown significantly higher leakage from liposomes containing ergosterol (Matsumori et al., 2024). Future studies may focus on conducting a similar experiment with karmitoxin.

Overall, this study demonstrates that the hemolytic potential of karmitoxin parallels its cytotoxic potential. While lytic activities were also observed in the RTgill-W1 and HCEC-1CT cell lines, the LDH leakage was considerably low. This raises the question whether the

cytotoxic potential of karmitoxin is reversible when cells are exposed to a low concentration for a limited amount of time. Despite karmitoxin exhibiting a strong affinity towards ergosterol, cholesterol, and epicholesterol, a \pm 25 % modulation of (membrane) cholesterol could not affect cytotoxicity of the tested concentration (EC80). For a better understanding of the role of membrane sterols on the MOA of karmitoxin an assessment of lytic activity against liposomes with various lipid profiles is needed. In addition, assessing the impact on cellular mechanisms, such as disruption of cell signaling pathways, oxidative stress, or osmoregulation, is crucial for providing a more comprehensive picture of the MOA of karmitoxin. Another interesting aspect to evaluate is the influence of karmitoxin on the membrane permeability to Ca $^{2+}$, Na $^+$, and K $^+$.

CRediT authorship contribution statement

Hélène-Christine Prause: Writing – review & editing, Writing – original draft, Visualization, Methodology, Investigation, Funding acquisition, Formal analysis, Data curation, Conceptualization. Nadine Hochmayr: Writing – review & editing, Visualization, Investigation, Formal analysis, Data curation. Yanan Yu: Writing – review & editing, Visualization, Investigation, Formal analysis, Data curation. Thomas Ostenfeld Larsen: Writing – review & editing, Resources, Methodology. Per Juel Hansen: Writing – review & editing, Resources, Methodology. Giorgia Del Favero: Writing – review & editing, Supervision, Resources, Methodology, Conceptualization. Doris Marko: Writing – review & editing, Supervision, Resources, Funding acquisition. Allen Place: Writing – review & editing, Supervision, Resources, Methodology, Conceptualization. Elisabeth Varga: Writing – review & editing, Supervision, Resources, Project administration, Methodology, Funding acquisition, Conceptualization.

Declaration of competing interest

The authors declare that they have no known competing financial interests or personal relationships that could have appeared to influence the work reported in this paper.

Acknowledgements

Kristin Schirmer, Department of Environmental Toxicology, EAWAG, provided the RTgill-W1 cell line. The HCEC-1CT cell line was obtained from Jerry W. Shay from the UT Southwestern Medical Center. We want to acknowledge Michael Murphy, Biacore, Cytiva (Danaher Corp., Washington DC, USA) who supported the data evaluation for SPR experiments. We are grateful to Peter Frühauf and the Department of Analytical Chemistry at the University of Vienna for the provision of the fluorescence detector. This work is partially supported by the USDA National Institute of Food and Agriculture through the Food Research Initiative SAS program (award #2021–68012–35922).

Funding

This research was supported by the University of Vienna, Faculty of Chemistry, Department of Food Chemistry and Toxicology, and was partly funded by the travel grant of the Doctoral School in Chemistry (DoSChem) of the University of Vienna. Open access funding was provided by the University of Veterinary Medicine Vienna. This research was funded in whole or in part by the Austrian Science Fund (FWF) [grant DOI: 10.55776/I5707]. For open access purposes, the corresponding author has applied for a CC BY public copyright license to any author accepted manuscript version arising from this submission.

Supplementary materials

Supplementary material associated with this article can be found, in the online version, at doi:10.1016/j.hal.2025.102817.

Data availability

Data will be made available on request.

References

- Axelsson, B.-O., Saraf, A., Larsson, L., 1995. Determination of ergosterol in organic dust by gas chromatography-mass spectrometry. J. Chromatogr. B 666, 77–84. https:// doi.org/10.1016/0378-4347(94)00553-H.
- Bergholtz, T., Daugbjerg, N., Moestrup, Ø., Fernández-Tejedor, M., 2006. On the identity of Karlodinium veneficum and description of Karlodinium armiger sp. nov. (Dinophyceae), based on light and electron microscopy, nuclear-encoded LSU RDNA, and pigment composition. J. Phycol. 42 (1), 170–193. https://doi.org/10.1111/ i.1529-8817.2006.00172.x.
- Binzer, S.B., Varga, E., Andersen, A.J.C., Svenssen, D.K., de Medeiros, L.S., Rasmussen, S. A., Larsen, T.O., Hansen, P.J., 2020. Karmitoxin production by Karlodinium armiger and the effects of K. armiger and karmitoxin towards fish. Harmful. Algae 99, 101905. https://doi.org/10.1016/j.hal.2020.101905.
- Bols, N.C., Barlian, A., Chirino-Trejo, M., Caldwell, S.J., Goegan, P., Lee, L.E.J., 1994. Development of a cell line from primary cultures of rainbow trout, *Oncorhynchus mykiss* (Walbaum), gills. J. Fish. Dis. 17 (6), 601–611. https://doi.org/10.1111/i.1365-2761.1994.tb00258.x.
- Brooks, G.A., Dubouchaud, H., Brown, M., Sicurello, J.P., Butz, C.E., 1999. Role of mitochondrial lactate dehydrogenase and lactate oxidation in the intracellular lactate shuttle. Physiology 96, 1129–1134. https://doi.org/10.1073/pnas.96.3.112.
- Deeds, J., Place, A., 2006. Sterol-specific membrane interactions with the toxins from Karlodinium micrum (Dinophyceae) — A strategy for self-protection? Afr. J. Mar. Sci. 28 (2), 421–425. https://doi.org/10.2989/18142320609504190.
- Deeds, J.R., Hoesch, R.E., Place, A.R., Kao, J.P.Y., 2015. The cytotoxic mechanism of karlotoxin 2 (KmTx 2) from Karlodinium veneficum (Dinophyceae). Aquatic Toxicology 159, 148–155. https://doi.org/10.1016/j.aquatox.2014.11.028.
- Deeds, J.R., Terlizzi, D.E., Adolf, J.E., Stoecker, D.K., Place, A.R., 2002. Toxic activity from cultures of Karlodinium micrum (=Gyrodinium galatheanum) (Dinophyceae)—A

- dinoflagellate associated with fish mortalities in an estuarine aquaculture facility. Harmful. Algae 1 (2), 169–189. https://doi.org/10.1016/S1568-9883(02)00027-6.
- Del Favero, G., Mayer, R.M., Dellafiora, L., Janker, L., Niederstaetter, L., Dall'Asta, C., Gerner, C., Marko, D., 2020. Structural similarity with cholesterol reveals crucial insights into mechanisms sustaining the immunomodulatory activity of the mycotoxin alternariol. Cells 9 (4), 847. https://doi.org/10.3390/cells9040847.
- Dufourc, E.J., 2008. Sterols and membrane dynamics. J. Chem. Biol. 1 (1–4), 63–77. https://doi.org/10.1007/s12154-008-0010-6.
- Fulda, S., Gorman, A.M., Hori, O., Samali, A., 2010. Cellular stress responses: cell survival and cell death. Int. J. Cell Biol. 2010, 214074. https://doi.org/10.1155/ 2010/214074.
- Garcés, E., Fernandez, M., Penna, A., Van Lenning, K., Gutierrez, A., Camp, J., Zapata, M., 2006. Characterization of new Mediterranean *Karlodinium* spp. (Dinophyceae) Strains using morphological, chemical, and physiological methodologies. J. Phycol. 42 (5), 1096–1112. https://doi.org/10.1111/j.1529-8817_2006.00270.x.
- Houdai, T., Matsuoka, S., Morsy, N., Matsumori, N., Satake, M., Murata, M., 2005. Hairpin conformation of amphidinols possibly accounting for potent membrane permeabilizing activities. Tetrahedron. 61 (11), 2795–2802. https://doi.org/ 10.1016/j.tet.2005.01.069.
- Lange, Y., Ye, J., Steck, T.L., 2004. How cholesterol homeostasis is regulated by plasma membrane cholesterol in excess of phospholipids. Proc. Natl. Acad. Sci. 101 (32), 11664–11667. https://doi.org/10.1073/pnas.0404766101.
- Matsumori, N., Hieda, M., Morito, M., Wakamiya, Y., Oishi, T., 2024. Truncated derivatives of amphidinol 3 reveal the functional role of polyol chain in sterolrecognition and pore formation. Bioorg. Med. Chem. Lett. 98, 129594. https://doi. org/10.1016/j.bmcl.2023.129594.
- Place, A.R., Bai, X., Kim, S., Sengco, M.R., Coats, D.W., 2009. Dinoflagellate host-parasite sterol profiles dictate karlotoxin sensitivity. J. Phycol. 45 (2), 375–385. https://doi. org/10.1111/J.1529-8817.2009.00649.X.
- Place, A.R., Ramos-Franco, J., Waters, A.L., Peng, J., Hamann, M.T., 2024. Sterolysin from a 1950s culture of *Karlodinium veneficum* (aka *Gymnodinium veneficum* Ballantine) forms lethal sterol dependent membrane pores. Sci. Rep. 14 (1), 17998. https://doi.org/10.1038/s41598-024-68669-0.
- Prause, H.C., Berk, D., Alves-de-Souza, C., Hansen, P.J., Larsen, T.O., Marko, D., Favero, G.Del, Place, A., Varga, E, 2024. How relevant are sterols in the mode of action of prymnesins? Aquat. Toxicol. 276, 107080. https://doi.org/10.1016/j. aquatox.2024.107080.
- Rasmussen, S.A., Binzer, S.B., Hoeck, C., Meier, S., De Medeiros, L.S., Andersen, N.G., Place, A., Nielsen, K.F., Hansen, P.J., Larsen, T.O., 2017. Karmitoxin: an amine-containing polyhydroxy-polyene toxin from the marine dinoflagellate *Karlodinium armiger*. J. Nat. Prod. 80 (5), 1287–1293. https://doi.org/10.1021/acs.instprod.6500860
- Rebhahn, V.I.C., Kiss, E., Marko, D., Del Favero, G., 2022. Foodborne compounds that alter plasma membrane architecture can modify the response of intestinal cells to shear stress in vitro. Toxicol. Appl. Pharmacol. 446, 116034. https://doi.org/ 10.1016/j.taap.2022.116034.
- Satake, M., Murata, M., Yasumoto, T., Fujita, T., Naoki, H., 1991. Amphidinol, a polyhydroxy-polyene antifungal agent with an unprecedented structure, from a marine dinoflagellate, *Amphidinium klebsii*. J. Am. Chem. Soc. 113 (26), 9859–9861. https://doi.org/10.1021/ja00026a027.
- Svendsen, M.B.S., Andersen, N.R., Hansen, P.J., Steffensen, J.F., 2018. Effects of harmful algal blooms on fish: insights from *Prymnesium parvum*. Fishes. 3 (1), 11. https://doi.org/10.3390/FISHES3010011.
- Svenssen, D.K., Binzer, S.B., Medić, N., Hansen, P.J., Larsen, T.O., Varga, E., 2019. Development of an indirect quantitation method to assess ichthyotoxic B-type prymnesins from *Prymnesium parvum*. Toxins 11 (5), 251. https://doi.org/10.3390/ toxins11050251
- Swasono, R.T., Mouri, R., Morsy, N., Matsumori, N., Oishi, T., Murata, M., 2010. Sterol effect on interaction between amphidinol 3 and liposomal membrane as evidenced by surface plasmon resonance. Bioorg. Med. Chem. Lett. 20 (7), 2215–2218. https://doi.org/10.1016/J.BMCL.2010.02.025.
- Van Wagoner, R.M., Deeds, J.R., Satake, M., Ribeiro, A.A., Place, A.R., Wright, J.L.C., 2008. Isolation and characterization of karlotoxin 1, a new amphipathic toxin from *Karlodinium veneficum*. Tetrahedron. Lett. 49 (45), 6457–6461. https://doi.org/ 10.1016/j.tetlet.2008.08.103.
- Waters, A.L., Oh, J., Place, A.R., Hamann, M.T., 2015. Stereochemical studies of the karlotoxin class using NMR spectroscopy and DP4 chemical-shift analysis: insights into their mechanism of action. Angew. Chem. 127 (52), 15931–15936. https://doi. org/10.1002/ange.201507418.
- Welch, W.J., 1993. How cells respond to stress. Sci. Am. 268 (5), 56–62. http://www.jstor.org/stable/24941478.